

# Hot Electron-Induced Electrogenenerated Chemiluminescence of Rare Earth(III) Chelates at Oxide-Covered Aluminum Electrodes<sup>1</sup>

S. Kulmala,<sup>2,4</sup> T. Ala-Kleme,<sup>2</sup> M. Latva,<sup>2</sup> K. Löikas,<sup>2</sup> and H. Takalo<sup>3</sup>

Received October 27, 1997; accepted February 27, 1998

Aromatic Gd(III) and Y(III) chelates produce ligand-centered emissions during cathodic pulse polarization of oxide-covered aluminum electrodes, while the corresponding Tb(III) chelates produce metal-centered  ${}^5D_4 \rightarrow {}^7F_6$  emissions. It was observed that a redox-inert paramagnetic heavy lanthanoid ion, Gd(III), seems to enhance strongly intersystem crossing in the excited ligand and direct the deexcitation toward a triplet-state emission, while a lighter diamagnetic Y(III) ion directs the photophysical processes toward a singlet-state emission of the ligand. The luminescence lifetime of Y(III) chelates was too short to be measured with our apparatus, but the luminescence lifetime of Gd(III) chelates was between 20 and 70  $\mu$ s. The mechanisms of the ECL processes are discussed in detail.

**KEY WORDS:** Oxide film; hot electron; hydrated electron; electrochemiluminescence; lanthanoid(III) chelates; gadolinium; yttrium.

## INTRODUCTION

Time-resolved electrogenerated chemiluminescence (tr-ECL) of aromatic Tb(III) chelates at thin insulating film-covered electrodes provides a means for extremely sensitive detection of Tb(III) and also of biologically interesting compounds, if aromatic Tb(III) chelates are used as labels in bioaffinity assays [1]. The high sensitivity is due mainly to the long luminescence lifetime of chelated Tb(III) and the use of time-resolved measuring

techniques in connection with pulsed excitation of chelates.

Transfer of hot electrons into aqueous electrolyte solutions has recently been reported to occur from metal/insulator/metal (M/I/M) junctions in contact with an electrolyte solution [2]. It is well-known that this kind of tunnel junction can act as a cold cathode and tunnel-emit hot electrons into vacuum [3]. Hot electrons have also been injected into insulating liquids, such as cyclohexane and benzene, at room temperature and into helium at low temperatures from Al/Al<sub>2</sub>O<sub>3</sub>/Au cold cathodes [4]. We have previously suggested that oxide-covered aluminum electrodes can act as cold cathodes and that the primary step in the above-mentioned tr-ECL is tunnel emission of hot electrons into the aqueous electrolyte solution [1,5]. The present ECL studies with Y(III) and Gd(III) chelates were conducted to elucidate further the ECL mechanisms of aromatic lanthanoid(III) chelates.

<sup>1</sup> Preliminary results of electrogenerated triplet-state emission of one of the ligands used in this work have been published in a letter elsewhere [9].

<sup>2</sup> Department of Chemistry, University of Turku, FIN-20014 Turku, Finland.

<sup>3</sup> Wallac Oy, P.O. Box 10, FIN-20101, Turku, Finland.

<sup>4</sup> To whom correspondence should be addressed. Fax: 358-2-3336700. e-mail: sakari.kulmala@utu.fi

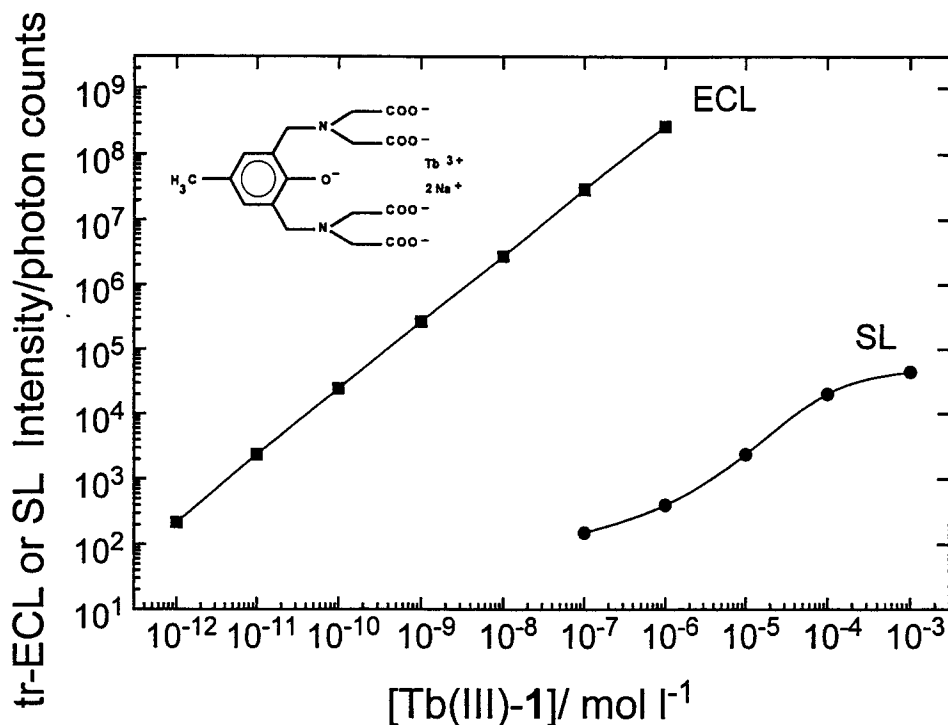


Fig. 1. Structure of Tb(III)-1 chelate and its calibration curves obtained by ECL and SL measurements. Conditions in ECL measurements: Al-cup/Pt-wire cell; 0.2 M boric acid buffer at pH 9.2; pulse charge, 120  $\mu\text{C}/\text{pulse}$ ; pulse frequency, 20 Hz; delay time, 50  $\mu\text{s}$ ; gate time, 8.0 ms; ECL intensity integrated over 5000 excitation cycles; and interference filter with a center wavelength of 546 nm and a transmission band half-width of about 10 nm. Conditions in SL measurements: 0.2 M boric acid buffer at pH 9.2; 20-kHz sonication; SL intensity integrated over 10 excitation bursts, each lasting 2.0 s; and 546-nm interference filter.

## EXPERIMENTAL

### Instrumentation and Reagents

The apparatus and methods of measurements have been described in detail elsewhere [1,5,6]. Briefly, ECL was excited either by a coulometric pulse generator [1] made in our laboratory or by a Pine Instruments RD4 potentiostat with a pulse generator made in our laboratory in a two-electrode cell, which was composed of either an Al-cup [6] working electrode and a Pt-wire counterelectrode or an Al-plate working electrode in a 1-cm spectrophotometer cuvette with a Pt-wire counterelectrode. Al electrodes were cut from a 0.3-mm-thick Al band (Merck Art. 1057, batch 721 K4164557) and they were used as covered with a 2- to 3-nm-thick [7] natural oxide film. Light was detected with either a photon counting unit [6], a Nucleus MCS-scaler card attached to a PC, or a Perkin-Elmer LS-5 spectral luminometer.

$\text{TbCl}_3 \cdot 6\text{H}_2\text{O}$ ,  $\text{GdCl}_3 \cdot 6\text{H}_2\text{O}$ , and  $\text{YCl}_3 \cdot 6\text{H}_2\text{O}$  were products of Aldrich. Lanthanoid(III) ions were chelated

with either 2,6-bis[*N,N*-bis(carboxymethyl)aminomethyl]-4-methyl phenol or 2,6-bis[*N,N*-bis(carboxymethyl)aminomethyl]-4-benzoyl phenol. The ligands were obtained from Wallac Oy, Finland. These ligands act as 7-dentate chelators with rare earth(III) ions so that the phenolic hydroxyl group is deprotonated in the chelates in neutral and basic solutions.  $\text{K}_2\text{S}_2\text{O}_8$ , sulfuric acid, and  $\text{Na}_2\text{B}_4\text{O}_7 \cdot 10\text{-hydrate}$  were *pro analysi* products of Merck. Quartz-distilled water was used in all solutions.

## RESULTS AND DISCUSSION

### Basic Features of ECL

Tb(III) chelated by the ligand 2,6-bis[*N,N*-bis(carboxymethyl)aminomethyl]-4-methyl phenol (ligand 1) exhibits very strong ECL at oxide-covered aluminum electrodes during cathodic pulse polarization. This ECL allows us to detect Tb(III)-1 down to the picomolar level on a time-resolved basis (Fig. 1). Tb(III)-

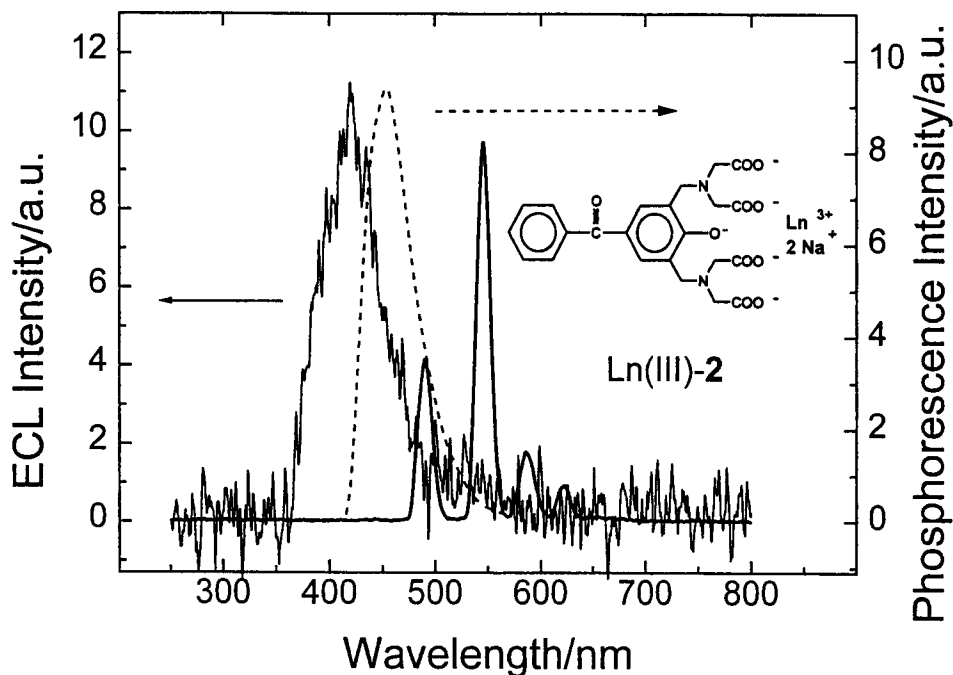


Fig. 2. ECL and frozen-state phosphorescence spectra of Gd(III)-2, ECL spectrum of Tb(III)-2, and structure of ligand 2. The ECL intensity of Tb(III)-2 is divided by a factor of 50. Conditions in ECL measurements: Al-plate/Pt-wire cell; Pine Instruments RD4 potentiostat; applied pulse voltage,  $-10$  V; pulse frequency, 100 Hz; pulse time, 200  $\mu$ s; 0.2 M boric acid buffer at pH 9.2; Perkin-Elmer LS-5; emission slit, 10 nm;  $1 \times 10^{-4}$  M Gd(III)-2 or  $1 \times 10^{-5}$  M Tb(III)-2. Conditions in phosphorescence measurements:  $1 \times 10^{-5}$  M Gd(III)-2; 77 K; 5:4 water-glycerol glass, pH 9.4; excitation wavelength, 320 nm; delay time, 0.10 ms; gate time, 5.0 ms; excitation slit, 15 nm; and emission slit, 5 nm.

1 also shows sonoluminescence (SL) [8] under conditions where hydroxyl radicals and hydrogen atoms are formed in the sonolysis of water, but the detection limit of the chelate is several orders of magnitude poorer (Fig. 1).

It has recently been demonstrated that (9-fluorenyl)methanol exhibits singlet-state emission when excited cathodically at oxide-covered aluminum electrodes by tunnel emission of hot electrons [5]. We have also shown in a letter that Gd(III) chelated by ligand 1 exhibits triplet-state emission of the ligand when the chelate is excited by injection of hot electrons from an oxide-covered aluminum electrode into an aqueous electrolyte solution [9]. When ligand 1 is replaced with 2,6-bis[*N,N*-bis(carboxymethyl)-aminomethyl]-4-benzoyl phenol (ligand 2), the Tb(III) chelate shows metal-centered  $^5D_4 \rightarrow ^7F_6$  emissions almost as strong as those of Tb(III)-1, but the ECL spectrum of Gd(III)-2 peaks at a shorter wavelength than the frozen-state phosphorescence spectra of Gd(III)-2 in aqueous glycerol glass at 77 K (Fig. 2). Previously, ECL and frozen-state phosphorescence spectra of Gd(III)-1 were observed to be identical [9].

Figure 3 displays the time spectra of intrinsic electrogenerated luminescence (IEL) of oxide-covered alu-

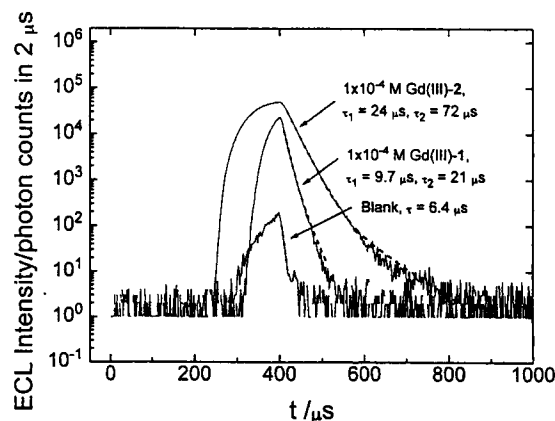


Fig. 3. Time profiles of ECL of Gd(III)-1 and Gd(III)-2 and IEL of the oxide-covered aluminum electrode. Conditions: Al-cup/Pt-wire cell; Pine Instruments RD4 potentiostat; applied pulse voltage,  $-10$  V; pulse frequency, 100 Hz; pulse time, 200  $\mu$ s; 0.2 M boric acid buffer at pH 9.2; MLS-2 scaler card; ECL integrated over 10,000 excitation pulses; and interference filter with a center wavelength of 405 nm and a transmission band half-width of about 10 nm.

minum electrodes and ECL of Gd(III)-1 and Gd(III)-2 chelates during excitation with voltage pulses lasting

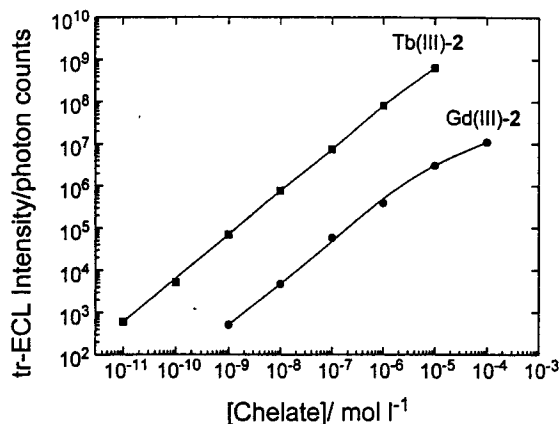


Fig. 4. Calibration curves of Tb(III)-2 and Gd(III)-2. Conditions as in the legend to Fig. 1, except the ECL intensity was integrated over 10,000 excitation cycles, and in the case of Gd(III)-2 the ECL was measured through a 405-nm interference filter, with a delay time of 1  $\mu$ s and a gate time of 1.0 ms.

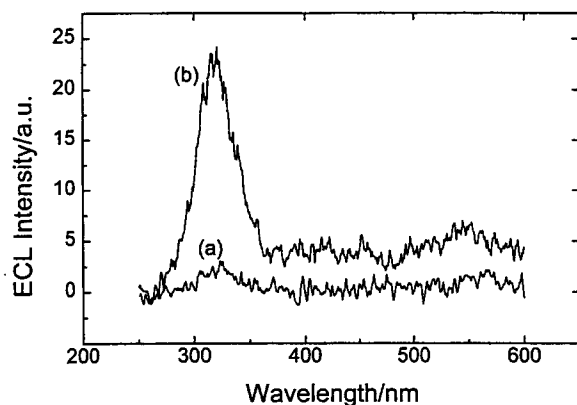


Fig. 5. ECL spectra of  $1.0 \times 10^{-5}$  M Y(III)-1 solution in the presence and absence of peroxydisulfate ions. Conditions: 0.2 M boric acid buffer at pH 9.2;  $1.0 \times 10^{-3}$  M  $K_2S_2O_8$ ; Pine Instruments RD4 potentiostat; applied pulse voltage, -10 V; pulse time, 200  $\mu$ s; pulse frequency, 100 Hz; Perkin-Elmer LS-5 spectroluminometer; emission slit, 20 nm; gate time, 13 ms; scanning speed, 240 nm/min.

200  $\mu$ s. The luminescence lifetime of Gd(III)-2 is about threefold that of Gd(III)-1, but the decays of the ECLs are clearly not single-exponential processes (Fig. 3) The tr-ECL of Tb(III)-2 and Gd(III)-2 also provides linear calibration curves spanning several orders of magnitude of concentration (Fig. 4).

When Y(III) is a central ion of the chelates, triplet-state emission is not seen, and singlet-state emission is observed instead (Fig. 5). The ECL intensity can be enhanced by the addition of peroxydisulfate ions as in the case of Tb(III) chelates [6,10] (Fig. 5). The ECL inten-

sity dependence on the chelate concentration was demonstrated with an ordinary spectral luminometer using Y(III)-2 and methods described elsewhere [5].

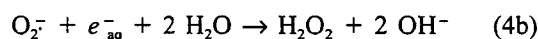
### Mechanisms of ECL

The general scheme of tunnel emission and Fowler-Nordheim tunneling of hot electrons into aqueous electrolyte solutions has been described elsewhere [5]. In principle, the cathodic reductions at oxide-covered aluminum electrodes could be due to direct action of hot dry electrons ( $e_{\text{quasifree}}^-$ ),  $e_{\text{aq}}^-$ , or heterogeneously transferred electrons from the bottom of the insulator conduction band or somewhere above it ( $e_{\text{CB}}^-$  of the insulator), and less energetic electrons via the surface states ( $e_{\text{SS}}^-$  of the insulator) [5].

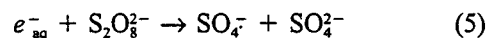


However, strong ECL of luminophores at oxide-covered aluminum electrodes has been observed only in the direct tunnel emission regime [5] (oxide film thickness, <4–6 nm), which implies that the  $e_{\text{quasifree}}^-$  or  $e_{\text{aq}}^-$  have an important role in the ECL pathways.

Under air-saturated solutions, and due to oxygen evolution at the counterelectrode, oxyradicals and hydrogen peroxide are formed, if hydrated electrons are produced at the working electrode.



with the second-order rate constants  $k_{4a} = 1.9 \times 10^{10}$  L mol<sup>-1</sup> s<sup>-1</sup>,  $k_{4b} = 1.3 \times 10^{10}$  L mol<sup>-1</sup> s<sup>-1</sup>, and  $k_{4c} = 1.2 \times 10^{10}$  L mol<sup>-1</sup> s<sup>-1</sup>, respectively [11]. The oxygen concentration of air-saturated electrolyte solutions is close to  $2 \times 10^{-4}$  M. [12]. If coreactants such as hydrogen peroxide (4c) or peroxydisulfate ions (5) are added, strongly oxidizing radicals are directly cathodically generated ( $k_5 = 1.2 \times 10^{10}$  L mol<sup>-1</sup> s<sup>-1</sup>) [11]:



Peroxydisulfate ion produces, by one-electron reduction, a strongly oxidizing sulfate radical (5) [ $E^\circ(SO_4^{\cdot-}/SO_4^{2-}) = 3.4$  V] [13], which can rapidly oxidize aromatic compounds including benzene [14]. The production of a sulfate radical was also essential for the ECL of (9-fluorenyl)methanol in air-saturated solutions, because this compound yields ECL mainly by the oxidation-in-

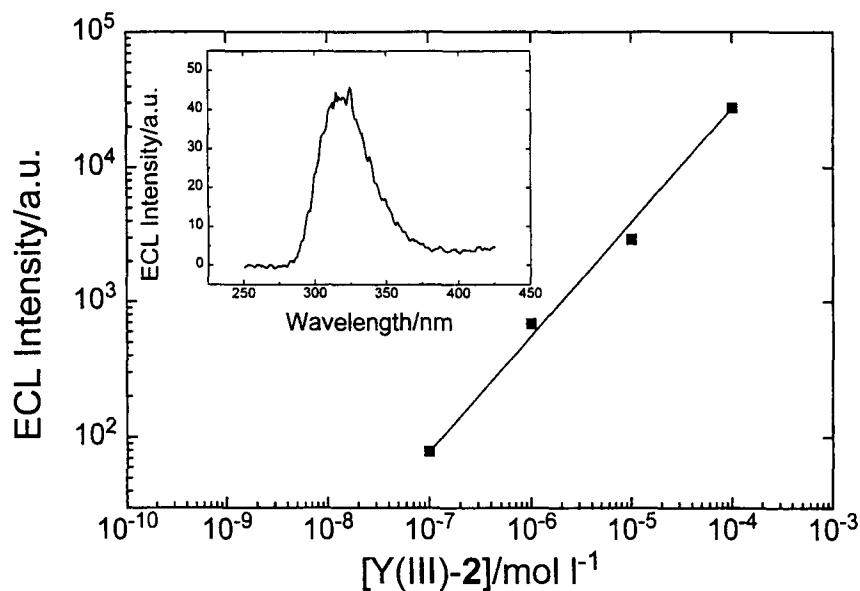


Fig. 6. ECL spectrum of  $1 \times 10^{-5}$  M Y(III)-2 solution and calibration curve of Y(III)-2. Conditions as in the legend to Fig. 5, except 0.2 M borate buffer adjusted to pH 7.8 with sulfuric acid,  $1 \times 10^{-3}$  M  $K_2S_2O_8$ . The calibration curve was measured with a Perkin-Elmer LS-5 integrating ECL signal 200 s from the beginning of the pulse polarization; emission wavelength, 320 nm; emission slit, 20 nm.

initiated reductive ECL pathway (ox-red pathway) and hydroxyl radicals cannot efficiently oxidize (9-fluorenyl)methanol [5,15]. However, phenolic compounds, especially phenoxides, are rapidly oxidized also by hydroxyl radicals [15], and hence the present luminophores can also be excited in the absence of peroxydisulfate ions. However, converting the reducing equivalents of the system to oxidizing equivalents by reaction (5) usually enhances ECL at low or medium concentrations of peroxydisulfate ion and quenches ECL at higher concentrations (over 1–3 mM). This seems to occur generally in all ECL systems at thin insulating film-covered electrodes that require the simultaneous presence of a strong one-electron oxidant and a reductant. Y(III)-1, Y(III)-2, Gd(III)-1, and Gd(III)-2 emissions are strongly enhanced by the addition of peroxydisulfate ions to the sample solutions, which is shown in the case of Y(III)-1 in Fig. 5. However, the sulfate radical also induces cathodic F-center emission peaking at about 420 nm [16]. Hence, its enhancing effect is beneficial in the case of Y(III) chelates emitting at shorter wavelengths (Figs. 5 and 6) but not very useful in the case of the present Gd(III) chelates. In the absence of peroxydisulfate ions, the free radical scavengers quench the luminescence of the intrinsic emission centers of the oxide film only very weakly, but the ECL of the solvated luminophores efficiently, which demonstrates that lumi-

nophores are excited on the basis of charge transfer and not the energy transfer pathways [5,10,16].

Although hydroxyl radicals can be generated by the three-step reaction sequence (4a)–(4c), it is hard to accept that these reactions could produce sufficiently high amounts of hydroxyl radicals. Therefore, we believe that a parallel solid-state mechanism of generation of hydroxyl radicals exists involving charge transfer via the anion vacancies with trapped electron centers as intermediates [9,17], analogously to that suggested to occur at oxide-covered *n*-silicon electrodes [18].

We have previously studied chemiluminescence (CL) of aromatic Tb(III) chelates induced by hydrated electrons in the presence of hydroxyl radicals [19], dichlorine radical ions [20], or sulfate radicals [21]. In this CL the ligand is usually first oxidized by a one-electron process and then reduced by a hydrated electron, with the result that the ligand is in the original oxidation state but now in its electronically excited state [19–21]. After this the excitation energy is transferred intramolecularly to the central ion, which finally emits metal-centered emissions. An analogous ligand-sensitized CL mechanism has also been proposed for the ECL of aromatic Tb(III) chelates, occurring at cathodically pulse-polarized aluminum electrodes [1,10].

In the present cases, central ions Y(III) and Gd(III) do not have excited states below the triplet states of the

ligands, and hence energy transfer to the central ion cannot occur [22,23], and deexcitation of the ligand can occur either nonradiatively or by the radiative transitions of the ligand which are actually experimentally observed. The luminescence lifetime of the ECL of Gd(III)-1 and Gd(III)-2 in aqueous solutions is of the order of tens of microseconds (Fig. 3), while the luminescence lifetimes of Y(III)-1 and Y(III)-2 chelates are too short to be measured with our apparatus and cell.

The present ECL spectra demonstrate that the excitation step of ECL of Ln(III)-1 chelates must have  $-\Delta G > \text{ca. } 4.3 \text{ eV}$  and  $-\Delta H \text{ ca. } 0.1\text{--}0.2 \text{ eV}$  higher [24], i.e., close to 4.5 eV. The intrinsic cathodic EL of the oxide film is so weak above 4 eV that it can be reliably observed only by the single-photon counting technique and cannot have a strong contribution to the excitation of the present luminophores. Because aromatic Ln(III) chelates can be used as electrochemiluminescent labels in immunometric immunoassays [1], i.e., label molecules can be excited at least several tens of nanometers away from the electrode surface, and because of the high energy required for the excitation step, the excitation mechanism in aqueous solutions must involve radical species which are capable of mediating in the redox steps of excitation pathways well beyond the distances possible for electron tunneling in solution.

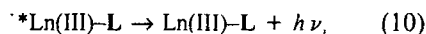
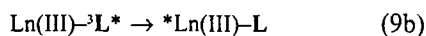
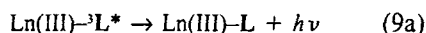
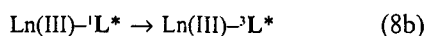
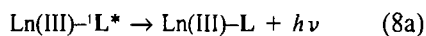
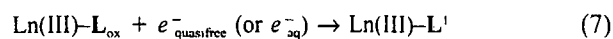
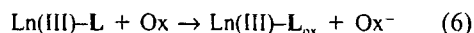
It is suggested that in the present case ligand 1 is excited predominantly by an ox-red pathway due to the high oxidation rate of phenoxides with hydroxyl radicals and the low reactivity of phenoxides with hydrated electrons and better stability of cation radicals than anion radicals of phenoxides as discussed elsewhere in the cases of Tb(III)-1 and Gd(III)-1 [9,20]. Ligand 2 certainly reacts rapidly with hydrated electron [ $k(e_{\text{aq}}^- + \text{benzophenone}) = 1.0 \times 10^{10} \text{ L mol}^{-1} \text{ s}^{-1}$ ] [11], and hence, a ligand reduction-initiated oxidative excitation pathway (red-ox pathway) could also be possible [20]. However, the luminescence lifetimes of the ECL of Tb(III)-1 and Tb(III)-2 are equal, ca. 2.2 ms at pH 9.2, and the photoluminescence (PL) lifetime of Tb(III)-1 is also the same as the ECL lifetime, but the PL lifetime of Tb(III)-2 is exceptionally short, below 0.2 ms [1]. When the carbonyl group from Tb(III)-2 is reduced to a hydroxyl group with sodium borohydride in aqueous solutions, the PL lifetime increases as the reduction proceeds and finally reaches 2.2 ms [1]. The ECL spectrum of Gd(III)-2 peaks at a wavelength about 30 nm lower than the solid-state phosphorescence spectrum (Fig. 4). On this basis, it is concluded that Ln(III)-2 emission is never predominant in the ECL process, but ligand 2 is first rapidly reduced to a hydroxyl derivative 2-OH, which

has lost the conjugation between the benzene rings and has photophysics and reactivity very similar to those of ligand 1. This is in accordance with the observed difference in the emission maxima of ECL and solid-state phosphorescence induced by Gd(III)-2 (Fig. 4). In addition, long-term cathodic pulsing at oxide-covered aluminum electrodes transforms the absorption spectra of Ln(III)-2, shifting the absorption maximum from 320 to about 300 nm. Thus, it is concluded that in the case of ECL of Ln(III)-2, the main emitting species is Ln(III)-2-OH.

Gadolinium(III) is the most redox inert ion in the whole lanthanide series [with  $E^\circ(\text{Gd}^{4+}/\text{Gd}^{3+}) = 7.9 \text{ V}$  and  $E^\circ(\text{Gd}^{3+}/\text{Gd}^{2+}) = -3.9 \text{ V}$ ] [22] due to its half-filled f-shell, while the closed-shell lanthanoid ion Y(III) is certainly impossible to oxidize in aqueous solutions. The oxidation potential of 1 is assumed to be ca. 0.8 V, i.e., close to that of the phenoxide ion, and the reduction potential is estimated to be ca. -2.6, i.e., the reduction potential must be less negative than the redox potential of the hydrated electron because 4-methyl phenol is relatively sluggishly reduced by the hydrated electron [11,20].

One-electron reductions of Gd(III) and Y(III) have been claimed to occur in aqueous solutions [ $k(\text{Gd(III)} + e_{\text{aq}}^-) = 5.5 \times 10^8 \text{ M}^{-1} \text{ s}^{-1}$ ,  $k(\text{Y(III)} + e_{\text{aq}}^-) = 2 \times 10^8 \text{ M}^{-1} \text{ s}^{-1}$ ] [11]. However, the purification of lanthanides and lanthanoids is very difficult, and even traces of easily reducible members of the Ln(III) series, such as Eu(III) and Yb(III), can induce considerable errors in the measured rate constants. The chelation of even highly reactive Ln(III) ions such as Eu(III) and Yb(III) by EDTA-type ligands [25a] strongly decreases the reduction rates of Ln(III) ions, and low reduction rate constants have been obtained for EDTA-chelated ions even in the studies in the early 1960s using relatively impure lanthanoid salts [ $k(\text{Gd}^{\text{III}}(\text{EDTA}) + e_{\text{aq}}^-) = 6 \times 10^6 \text{ M}^{-1} \text{ s}^{-1}$  and  $k(\text{Y}^{\text{III}}(\text{EDTA}) + e_{\text{aq}}^-) = 1.1 \times 10^7 \text{ M}^{-1} \text{ s}^{-1}$ ] [25b]. Probably, these rate constants are erroneously high as discussed previously in the case of Gd(III) [9].

On the above basis, the red-ox excitation pathway cannot be significant in the present cases if the hydrated electron is the main reducing mediator, and also, the reduction (and oxidation) of Y(III) and Gd(III) can be neglected. Moreover, if appropriate concentrations of peroxydisulfate ions are added to the samples, the ox-red excitation pathway is even more favored due to the high second-order rate constant of reduction of peroxydisulfate ion [5]. Thus, the following excitation scheme is applicable:



where L is either ligand 1 or ligand 2-OH and Ox $\cdot$  is a hydroxyl or sulfate radical. According to the present results it seems that the ligand is predominantly excited to its lowest excited singlet state in reaction [7] and no evidence of direct excitation to the ligand triplet state [10,20] was obtained; only singlet-state emission of the ligand is observed in the ECL spectra of Y(III)-1 or Y(III)-2 (Figs. 4 and 5) (8a). When Gd(III) is the central ion, only ligand triplet-state emission is observed (9a) (Fig. 4 and Fig. 1 in Ref. 9), which implies that Gd(III) can very efficiently enhance intersystem crossing (8b) in the ligand. On the other hand, Tb(III) ion also enhances intersystem crossing but can also accept energy from the ligand triplet state to its resonance level (9b), finally showing metal-centered emissions  ${}^5\text{D}_4 \rightarrow {}^7\text{F}_j$  [10].

The present results support the ECL and CL mechanisms proposed previously [1,10,19-21] in the case of aromatic Tb(III) chelates, but do not unequivocally show to what extent the energetic reductions are based on the reactions of dry hot electrons and, on the other hand, on the reactions of hydrated electrons. If the estimated [9,20] redox potentials for ligand 1 in aqueous solutions are sufficiently accurate, the ox-red excitation pathway resulting in the singlet-state emission of the ligand must involve a more energetic electron than the hydrated electron (see energy diagram in Fig. 2 in Ref. 9). If the presolvated hot electron is the main reducing species, the red-ox excitation pathway can also be energetically possible, but the anion radical of the ligand remains highly unstable [20]. This fact gives greater support for the ox-red excitation pathway. An interesting point in the present results is that a paramagnetic heavy lanthanoid ion, Gd(III), seems strongly to enhance intersystem crossing in the excited ligand and direct the deexcitation toward a triplet-state emission, while a lighter diamagnetic Y(III) ion directs the photophysical processes toward a singlet-state emission of the ligand. Experiments

using several metal/oxide/electrolyte tunnel emitters and other redox inert lanthanoid(III) ions of different molecular weights are in progress in our laboratory.

## REFERENCES

1. S. Kulmala, Academic dissertation, Finland, Turku, 1995.
2. D. Diesing, S. Russe, A. Otto, and M. Lohrengel (1995) *Ber. Bunsenges. Phys. Chem.* **99**, 1402-1405; S. Kulmala and T. Ala-Kleme (1997) *Ber. Bunsenges. Phys. Chem.* **101**, 758-761; D. Diesing, G. Krizler, and A. Otto (1997) *Ber. Bunsenges. Phys. Chem.* **101**, 761-764.
3. C. Mead (1961) *J. Appl. Phys.* **32**, 646-652; E. Savoye and D. Anderson (1967) *J. Appl. Phys.* **38**, 3245-3265; J. Drucker and P. Hansma (1984) *Phys. Rev. B* **30**, 4348-4350.
4. M. Silver, D. Onn, P. Smejtek, and K. Masuda (1967) *Phys. Rev. Lett.* **19**, 626-630.
5. S. Kulmala, T. Ala-Kleme, L. Heikkilä, and L. Väre, *J. Chem. Soc. Faraday Trans.* (in press).
6. J. Kankare, K. Fälden, S. Kulmala, and K. Haapakka (1992) *Anal. Chim. Acta* **256**, 17-28.
7. A. Despić and V. Parkhutik (1989) in J. Bockris, R. White, and B. Conway (Eds.), *Modern Aspects of Electrochemistry, Vol. 20*, Plenum Press, New York, pp. 400-503 (and references cited therein).
8. S. Kulmala, T. Ala-Kleme, M. Latva, and K. Haapakka (1996) *J. Chem. Soc. Faraday Trans.* **92**, 2529-2533.
9. S. Kulmala and T. Ala-Kleme (1997) *Anal. Chim. Acta* **355**, 1-5.
10. S. Kulmala and K. Haapakka (1995) *J. Alloys Compd.* **225**, 502-506.
11. G. Buxton, C. Greenstock, W. Helman, and A. Ross (1988) *J. Phys. Chem. Ref. Data* **17**, 513-886 (and references cited therein).
12. W. Koppenol and J. Butler (1985) *Adv. Free Rad. Biol. Med.* **1**, 91-131.
13. R. Memming (1969) *J. Electrochem. Soc.* **116**, 785-790.
14. P. Neta, R. Huie, and A. Ross (1988) *J. Phys. Chem. Ref. Data* **17**, 1027-1284 (and references cited therein).
15. S. Steenken (1996) *Top. Curr. Chem.* **177**, 125-145; S. Steenken (1987) *J. Chem. Soc. Faraday Trans. I* **83**, 113-124.
16. S. Kulmala, T. Ala-Kleme, A. Hakonen, and K. Haapakka (1997) *J. Chem. Soc. Faraday Trans.* **93**, 165-168.
17. S. Kulmala, A. Kulmala, M. Helin, and I. Hyppänen (1998) *Anal. Chim. Acta* **359**, 71-86.
18. T. Ala-Kleme, S. Kulmala, and M. Latva (1997) *Acta Chem. Scand.* **51**, 541-546.
19. S. Kulmala, A. Hakonen, E. Laine, and K. Haapakka (1995) *J. Alloys Compd.* **225**, 279-283.
20. S. Kulmala, A. Kulmala, M. Latva, and K. Haapakka, *Anal. Chim. Acta* (in press).
21. S. Kulmala, P. Raerinne, H. Takalo, and K. Haapakka (1995) *J. Alloys Compd.* **225**, 492-496.
22. W. Carnall (1979) in K. Gschneider, Jr., and L. Eyring, (Eds.), *Handbook on the Physics and Chemistry of Rare Earths, Vol. 3*, North-Holland, Amsterdam, pp. 171-208.
23. P. Sammes and G. Yahiloglu (1996) *Nat. Prod. Rep.* **13**, 1-27.
24. L. Faulkner, H. Tachikawa, and A. J. Bard (1972) *J. Am. Chem. Soc.* **94**, 691-699.
25. E. J. Hart and M. Anbar (1970) *The Hydrated Electron*, John Wiley & Sons, New York, (a) p. 283, (b) pp. 100-103.